

Study of Catalytic Pyrolysis of Biomass Sorghum (*Sorghum bicolor* L. Moench) Using Design of Experiments and Surface Response Methodology

Diego M. Costa,^a Maria L. F. Simeone,[✉]*^b Rafael A. C. Parrella^b and Isabel C. P. Fortes^a

^aDepartamento de Química, Instituto de Ciências Exatas (ICEx), Universidade Federal de Minas Gerais, Av. Pres. Antônio Carlos, 6627, 31270-901 Belo Horizonte-MG, Brazil

^bEmbrapa Milho e Sorgo, Rodovia MG 424, km 45, 35701-970 Sete Lagoas-MG, Brazil

This study proposes a screen of variables that have an influence on the modification of the bio-oil chemical composition as a unique critical quality attribute (CQA) throughout the pyrolytic process (zeolite, ZSM-5) by using a 2⁴ full factorial design, followed by optimization through a response surface methodology (RSM) based on central composite design (CCD) involving samples of biomass sorghum BRS716 (*Sorghum bicolor* L. Moench). The pyrolysis of pure biomasses and the biomass impregnated with the catalyst was carried out in a vertical bench furnace at 500 °C. Screening design involved factor variation in two levels (-1 and +1) of four variables as critical process parameters (CPPs) such as furnace heating rate (°C min⁻¹), nitrogen flow (mL min⁻¹), amount of biomass (g), and catalyst (% m/m), leading to obtaining bio-oil. Thus, it was possible to create a response surface from these two variables (biomass and catalyst), in which a minimum critical point was reached. The production of a bio-oil rich in hydrocarbon compounds is possible, but a large amount of catalyst was required. Two analytical techniques based on gas chromatography coupled to mass spectrometry (GC-MS) and mid-infrared (MIR) spectroscopy, provided additional information to fully characterize bio-oil chemical composition.

Keywords: pyrolytic process, biofuels, bio-oil, optimization, response surface methodology

Introduction

Biomass products have received increasing attention since they efficiently provide energy and reduce greenhouse gases. In addition to being a source of food and renewable energy, biomass also provides raw materials for the chemical industry.¹ Lignocellulosic biomass is a plant material formed by complex organic macromolecules such as polysaccharides (cellulose and hemicellulose) and lignin, responsible for its structure.²⁻⁶ Thus, this biomass cannot be defined as a single chemical substance but rather as a class of related materials, as they present complex structures and variable compositions.

Sorghum (*Sorghum bicolor* L. Moench) is lignocellulosic biomass of tropical origin grown from seeds. Its study is of great interest once it has an appreciable amount of sugar, greater resistance to drought and temperature, and reaches maturity in a short time when compared to other species such as maize, soybean, and wheat.⁷ It is considered a

crop with universal value as it can be grown in tropical, subtropical, temperate, and semiarid regions. It is adaptable to existing cropping systems, can serve as a secondary or short-cycle crop, and is used as a source of forage and silage for livestock production systems.⁸ In addition, it has an extensive root system that contributes to the accumulation of soil organic carbon after plant shoot removal. It can alleviate concerns about soil organic matter depletion resulting from straw removal.⁷

There are different types of sorghum: grain, forage, saccharine, broom, and high biomass, which are classified according to their use.⁷ The biomass sorghum used in this study is a new hybrid developed by researchers in Brazil at Embrapa Milho e Sorgo. Sorghum cultivation is favored by seed propagation, which facilitates the implementation of new areas.^{9,10} These characteristics make sorghum a crop with great potential in the production of biofuels, such as the production of second-generation ethanol.¹¹

One of the ways to convert biomass for its use as fuel is its secondary conversion through thermal treatment, called pyrolysis, which generates both liquids (bio-oil), gaseous (CO, CO₂, H₂O, and light hydrocarbons) and

*e-mail: marialucia.simeone@embrapa.br

Editor handled this article: Rodrigo A. A. Muñoz (Associate)

solids (bio-coal) products.¹² Pyrolysis has some advantages over other conversion methods, such as low-temperature requirements, inert atmosphere conditions, and production of a high-quality bio-oil.¹³ The synthesis of bio-oil has been the subject of several studies since it has a high energy density, low toxicity, lower nitrogen and sulfur content, and is easily stored, transported, and used.¹² Bio-oil can still be subsequently transformed into fuels such as diesel and gasoline or be used as antioxidants, phenolic resins, solvents, wood preservatives, monomers for plastics, etc., according to the constitution of lignocellulosic biomass.^{14,15} However, it also has undesirable properties, such as high water content, viscosity, ash content, low calorific value, instability, and high corrosivity, limiting industrial applications.¹⁶

Therefore, when it is used as a transport fuel or as raw material, it is necessary to improve its properties, which is called “upgrading”.¹⁷ There are several techniques that have been developed for this purpose, such as ash removal in the feedstock, hydrogenation, catalytic cracking, catalytic pyrolysis, molecular distillation, steam reforming, supercritical fluids, esterification, and emulsification.¹⁸ The use of a catalyst during the pyrolysis process (catalytic pyrolysis) will lead to the deoxygenation process of the biomass with the breakdown/transformation of the oxygenated intermediates.¹⁹ The catalyst can be directly mixed with the biomass, a process which is known as *in situ*, or mixed only with the pyrolysis vapors, *ex situ*.²⁰ Fast catalytic pyrolysis has a great potential to produce hydrocarbons directly from biomass or produce bio-oils with better quality and higher stability. Zeolites are a promising class of heterogeneous catalysts once they are tetrahedral crystalline materials consisting of SiO_4 and $[\text{AlO}_4]^-$, in which the negative charge of $[\text{AlO}_4]^-$ is compensated by a cation (H^+), maintaining the overall neutrality of their structure.²¹ The charge compensation with H^+ makes them highly acidic, which is helpful for many catalytic applications.²² In their studies, Vichaphund *et al.*,²³ and Kim *et al.*,²⁴ showed that protonated zeolite (HZSM-5) favored the increase of hydrocarbons present in bio-oils from pyrolysis.

The design of experiments based on response surface methodology (RSM) in pyrolysis is also essential to optimize the best conditions for a process. It can reduce time, operating costs, yield improvement, and better agreement between the nominal values obtained and the desired values.²⁵ The use of factorial design allows determining which factors have relevant effects on the response and how the impact of one factor varies with the levels of the others.²⁵ In addition, it allows the interactions between the different factors to be measured. Among the multivariate analysis methods used for the simultaneous optimization of several variables, RSM is a set of statistical

and mathematical techniques useful for modeling and analyzing problems that include the effect of the interaction of related factors and the construction of empirical mathematical models.

Thus, this study aimed to perform an experimental design for pyrolysis with the factors oven heating rate, nitrogen flow, amount of sample, and amount of catalyst, to verify which conditions will give a better quality bio-oil. Pyrolysis was carried out in a vertical benchtop oven. The starting biomass was characterized by elemental and lignocellulosic analysis. The bio-oils were characterized using mid-infrared (MIR) spectroscopy; their chemical composition was determined using gas chromatography coupled to mass spectrometry (GC-MS).

Experimental

Samples and chemicals

Samples of BRS716, biomass sorghum (*Sorghum bicolor* L. Moench) were kindly provided by Embrapa Milho e Sorgo, located in the city of Sete Lagoas-MG and referred to the harvest of the first semester of 2015. The samples were previously milled in a Wiley mill for the obtention of smaller and more uniform particle sizes. Furthermore, they were oven dried at 105 °C to remove any moisture. The chemicals used to prepare the neutral detergent solution were: anhydrous sodium phosphate 99% m/m (Sigma-Aldrich, Campinas, Brazil); sodium tetraborate (borax) decahydrate 99-105% m/m (Sigma-Aldrich, Campinas, Brazil); anhydrous sodium phosphate 99% m/m (Sigma-Aldrich, Campinas, Brazil); ethylenediaminetetraacetic acid disodium salt dihydrate (EDTA) 99-101% m/m, (Sigma-Aldrich, Campinas, Brazil); ethylene glycol (Sigma-Aldrich, Campinas, Brazil). To prepare the detergent solution acid: sulfuric acid (Sigma-Aldrich, Campinas, Brazil); and cetyl trimethyl ammonium bromide (CTAB) 99% m/m (Sigma-Aldrich, Campinas, Brazil), H_2SO_4 solution 72% (m/v) (Vetec, Duque de Caxias, Brazil); chloroform P.A. (Vetec, Duque de Caxias, Brazil) were also used.

Zeolite ZSM-5 (Sigma-Aldrich, Campinas, Brazil), with a $\text{SiO}_2/\text{Al}_2\text{O}_3$ ratio, 23 wt.% of 0.05% Na_2O , and a surface area of 425 $\text{m}^2 \text{g}^{-1}$ was used. Before using it, the zeolite was calcined at 550 °C for 5 h to increase its acidity.

Biomass characterization

Elemental analysis

The elemental composition of the sorghum biomass BRS716 sample was measured with CHNS/O Elemental

Analyzer (PerkinElmer 2400 Series II, PerkinElmer Inc., Waltham, MA, USA). Two to 3 mg (accurate to 0.001 mg) of the ground sample were weighed into tin capsules using a Shimadzu ATY-224 balance (Shimadzu Corporation, Kyoto, Japan). The ground sample was packed with foil, introduced into the combustion chamber through a funnel, burned under a pure oxygen atmosphere, and detected by a thermoconductometer detector.

The percentage of oxygen was estimated by difference ($100 - (C + H + N)$). Elemental compositions were reported as a percentage of initial dry weight (m/m, db).

Determination of cellulose, hemicellulose, and lignin content

Cellulose, hemicellulose, and lignin contents of the raw biomass were determined based on the sequential extraction method developed by van Soest *et al.*,²⁶ with the improvement of the technique using a new system called Ankom (filter bag technique of Ankom®, FBT).

Approximately 0.5 g of each sample was placed in filter bags (F57) and sealed by heating using a sealing machine (Ankom, Macedon, USA). The filters with samples were heated in a neutral detergent solution. The cell contents were solubilized in this process while filtration separated the insoluble cell wall (cellulose, hemicellulose, and lignin). Filters with neutral detergent fiber (NDF) residues were dried at 105 °C using an oven (American Lab, San Francisco, USA) and weighed using a Shimadzu ATY-224 balance (Shimadzu Corporation, Kyoto, Japan) to determine the NDF content. They were then subjected to heating with the acid detergent solution. In this process, hemicellulose was solubilized, and the new residue (consisting almost entirely of lignin and cellulose) was dried at 105 °C and weighed to determine the acid detergent fiber (ADF) content. The ADF residue was subjected to a 72% (m/v) sulfuric acid (Vetec, Duque de Caxias, Brazil) solution for 3 h for lignin estimation. Filters with residues resulting from this procedure were dried at 105 °C and weighed to determine lignin. Subsequently, the residues were ignited at 500 °C using a muffle furnace (Tecnal, Piracicaba, Brazil) for 4 h to assess the residual ash. The amount of cellulose was determined by the difference between ADF and lignin, and the hemicellulose content was found as the difference between NDF and ADF.

Thermogravimetric analysis (TG) and derivative thermogravimetric analysis (DTG)

Sorghum samples and their mixtures with the catalyst (5, 10, 15, and 20% (m/m)) were subjected to thermogravimetric analysis on the equipment TGA-Q50 (TA Instruments, New Castle, USA). A platinum crucible was used. About 30 g of the samples were submitted to

a heat treatment from room temperature to 800 °C at 10 °C min⁻¹. Nitrogen was used as a purge gas with a 40 mL min⁻¹ flow rate at the side and 60 mL min⁻¹ at the upper oven inlet. The TG and DTG curves were obtained using the TA Instruments Operating Software (TA Instruments, New Castle, USA).

Experimental design

A 2⁴ complete factorial design with three central points was used in this study. The factors used to produce bio-oil were studied with standard RSM to identify and optimize the effective process parameters. With this method, a core factorial forms a cube with sides of two coded units in length (from the up +1). Table 1 shows the ranges and the levels of the variables examined and their combinations in this study. The studied variables were pyrolysis furnace heating rate (X_1), nitrogen flow (X_2), amount of biomass (X_3), and amount of catalyst (X_4). The experimental sequence was randomized to minimize the effects of the uncontrolled factors. The response factor for this experimental design was the hydrocarbon content in bio-oil. Table 2 shows the number of each experiment, coded and actual values of variables.

Table 1. Variables used in the design of experiments

Variable	Name	Variable level		
		-1	0	+1
X_1	furnace heating rate / (°C min ⁻¹)	100	150	200
X_2	nitrogen flow / (mL min ⁻¹)	100	200	300
X_3	biomass amount / g	5	10	15
X_4	catalyst amount / (% m/m)	5	17.5	30

Fast pyrolysis on bench scale

Pyrolysis was performed in a stainless steel Fortelab tubular vertical furnace, FT-1200 H / V (FORTELAB - Indústria de Fornos Elétricos Ltda, São Carlos, Brazil) with an inside diameter of 6 and 45 cm in length, in which a glass reactor was inserted for sample insertion. Figure S1 (Supplementary Information section) shows the assembly for the execution of pyrolysis.

The samples were transferred to the glass reactor 45 cm in length and two inlets for the nitrogen flow. The glass reactor was placed into the tubular vertical furnace. The glass reactor was connected to a straight condenser and a round bottom flask to collect the condensable compounds (water and bio-oil). The latter, in turn, was coupled to a condenser to retain the most significant amount of the liquid fraction. Finally, two traps are connected sequentially and filled with water, kept cooler to recover the non-condensable. The furnace was programmed as

Table 2. Design of experiments for bio-oil production from biomass sorghum

Experiment	Coded variables				Real values			
	$X_1 / (^\circ\text{C min}^{-1})$	$X_2 / (\text{mL min}^{-1})$	X_3 / g	$X_4 / (\% \text{ m/m})$	$T / ^\circ\text{C}$	Flow / (mL min^{-1})	w / g	w / %
1	-1	-1	-1	-1	100	100	5	5
2	1	-1	-1	-1	200	100	5	5
3	-1	-1	1	-1	100	100	15	5
4	1	-1	1	-1	200	100	15	5
5	-1	-1	-1	1	100	100	5	30
6	1	-1	-1	1	200	100	5	30
7	-1	-1	1	1	100	100	15	30
8	1	-1	1	1	200	100	15	30
9	-1	1	-1	-1	100	300	5	5
10	1	1	-1	-1	200	300	5	5
11	-1	1	1	-1	100	300	15	5
12	1	1	1	-1	200	300	15	5
13	-1	1	-1	1	100	300	5	30
14	1	1	-1	1	200	300	5	30
15	-1	1	1	1	100	300	15	30
16	1	1	1	1	200	300	15	30
17	0	0	0	0	150	200	10	17.5
18	0	0	0	0	150	200	10	17.5
19	0	0	0	0	150	200	10	17.5

X_1 : furnace heating rate; X_2 : nitrogen flow; X_3 : biomass amount; X_4 : catalyst amount; T: temperature; w: weight.

follows: heating rate of 100-200 $^\circ\text{C min}^{-1}$ until reaching a temperature of 450 $^\circ\text{C}$ (20 min). For system cooling: a cooling rate of 100 $^\circ\text{C min}^{-1}$ until reaching a temperature of 80 $^\circ\text{C}$. The nitrogen flow was adjusted according to experiments shown in Table 2. The temperature profile in the glass reactor was measured with two thermocouples, one device vertically in the center of the tubular furnace and another one horizontally disposed in the heating zone and outside the reactor, close to the resistances, and heating was controlled through software. After cooling the furnace and glass reactor, the residual material (the coals) obtained, known as “char”, was removed from the glass reactor and stored. The liquid (bio-oil) was separated from the aqueous phase by centrifugation and stored for later analysis.

Characterization of bio-oils

The chemical characterization of the bio-oils was performed by a Shimadzu GCMS-QP5050 device (Shimadzu Corporation, Kyoto, Japan) containing a PETROCOL capillary column (100 m \times 0.25 mm internal diameter \times 0.5 μm thickness). The oven temperature was initially programmed to 30 $^\circ\text{C}$ (10 min) and increased to 185 $^\circ\text{C}$ (75 min) at a rate of 2.5 $^\circ\text{C min}^{-1}$ and finally heated at a rate of 5 $^\circ\text{C min}^{-1}$ to 250 $^\circ\text{C}$ (53 min). Helium was used as a carrier gas with a flow rate of 0.8 mL min^{-1} . An aliquot

of 1 μL of the sample was injected. MS was operated in the electron impact ionization (EI) mode with an energy of 70 eV, and a range of m/z 45-500 was used for analysis. Peak identification was performed through the WILEY 07, NIST 08, NISTI 08S, NIST 05, and NIST 05S, present in the GC-MS Post-run Analysis library software. Retention times were also recorded. Those compounds that showed a degree of similarity higher than 85% were identified.

The bio-oils were analyzed by spectroscopy in the medium infrared region with transformed Fourier (MID-FTIR), in a wavenumber range of 4000-400 cm^{-1} , for the determination of the organic groups present in these samples using an FTIR equipment with ATR (attenuated total reflectance) diamond accessory for liquid samples and transmission cell for solid samples (ARIS-ZONE ABB Bomen, MB Series (Bomen, Quebec, Canada)). Solid samples were prepared in KBr pellets, and, for liquid samples, three drops were used for each analysis.

RSM

The responses and corresponding factors are modeled and optimized using RSM. The RSM technique is aimed at (i) design of experiments to provide adequate and reliable response measurements, (ii) developing a mathematical model having the best fit to the data obtained from the

experimental design, and (iii) determining the optimal value of the independent variables that produce maximum or minimum response values. Therefore, RSM was used to determine the optimum and experimental design matrix in this study specified according to the central composite design (CCD) method. For CCD, it is necessary to carry out a new design centered on the best experiments. In this case, we will work on the points 30% (m/m) and 15 g for the quantity of catalyst and biomass, respectively. When two variables are involved in CCD, the design is called a star. Star design consists of a complete or fractional two-level factorial design with a center point with more star drawing. In star design, the levels α (the same goes for any coded value x_i) need to be decoded for the experimental values of the levels of the variables to be studied.²⁷ Therefore, equation 1 is used:

$$X_{\text{cod}} = (X_{\text{real}} - \text{PC}) / (\Delta X / 2) \quad (1)$$

where X_{cod} = coded value, X_{real} = real value, PC = real value at the center point, ΔX = difference between the maximum real value and the center point. The correspondence between coded and correct values of the variables is listed in Table 3. Table 4 presents the design matrix used to construct the response surface using CCD. The values chosen were based on the preliminary results obtained in the design of the experiments.

Table 3. Values and levels of the variables used in the CCD

Variable	Variation levels				
	-1.41 ($-\alpha$)	-1	0	+1	1.41 ($+\alpha$)
Catalyst / (% m/m)	2	10	30	50	58
Biomass / g	1	5	15	25	29

α : the levels of the points of a factorial design are ± 1 and those on a "star" design are $\pm \alpha$, where $|\alpha| \geq 1$.

The response surface can be generated after processing the data in the Statistica 7.0 software developed by StatSoft.²⁸ The critical point, maximum or minimum produced by this curve, can be determined empirically. The quadratic model is the most adequate to describe the response surface's critical point since it can be adapted to various surfaces.²⁷ The polynomial model of a quadratic function is represented by two variables using equation 2.²⁷⁻²⁹

Table 5. Elemental and lignocellulosic composition of biomass sorghum BRS 716

Sample	C / %	H / %	N / %	O ^a / %	NDF / %	ADF / %	Hemicellulose / %	Cellulose / %	Lignin / %
Sorghum	41.40	4.30	0.20	54.1	70.48	44.49	25.99	37.95	6.54

^aO = 100 - C(%) - N(%) - H(%). C: carbon; H: hydrogen; N: nitrogen; O: oxygen; NDF: neutral detergent fiber; ADF: acid detergent fiber.

Table 4. Values and levels of the variables used to construct the response surface

Experiment	Catalyst	Biomass
1	-1	-1
2	1	-1
3	-1	1
4	1	1
5	0	0
6	0	1.41
7	0	-1.41
8	-1.41	0
9	1.41	0

Considering N_2 flow: 300 mL min⁻¹, furnace heating rate: 200 °C min⁻¹.

$$\hat{Y} = b_0 + b_1X_1 + b_2X_2 + b_{11}X_1^2 + b_{22}X_2^2 + b_{12}X_1X_2 \quad (2)$$

in which b_0 , b_1 , b_2 , b_{11} , b_{22} , and b_{12} are constants determined from matrix equations involving the variables X_1 , X_2 , and y_i (responses).

Coefficients of the models for one response were estimated with multiple regression analysis. The fit quality of the models was analyzed from their coefficients of correlation and determination. The adequacy of each model was also checked with the analysis of variance (ANOVA) using the Fisher F -test. This test determines the relationship between the response variable and a subset of the independent variables.

Results and Discussion

Characterization of biomass sorghum

The biomass sorghum was initially characterized for its hemicellulose, cellulose, and lignin contents and the carbon, nitrogen, and oxygen contents present in its structure. The oxygen composition was determined by subtracting the sum of carbon, hydrogen, and nitrogen percentages from 100%.^{30,31} The results obtained from this characterization are shown in Table 5.

Sorghum is a C4 plant belonging to the Poaceae family. Sorghum emerges as an alternative to the biomass supply chains for bioenergy and biorefining and has a high potential for biomass production.³¹⁻³³ Previous studies³⁴ reported that cellulose and hemicellulose contents varied

significantly with location, while lignin content remained relatively constant. According to Table 5, hemicellulose, cellulose, and lignin contents are close to the results found by de Oliveira *et al.*³⁴

The pyrolysis of the raw sorghum resulted in a product consisting of three fractions, that resulted in one liquid (condensed phase) 35.0% m/m, one gas (non-condensable phase) 35.0% m/m, and one solid (residual) 30.0% m/m.

TG and DTG analysis

TG and DTG of pure and impregnated sorghum with different proportions of zeolite (ZSM-5, 5-30% m/m) were performed to verify the mass loss behavior as a function of temperature (Figure 1) to choose the best temperature for pyrolysis. A similar degradation profile is observed in all cases, differing only in intensity at the maximum degradation peak and in the residual amount at the end of the process. As for pure biomass, they all presented two main stages of mass loss comprised in a temperature range of 165-205 and 260-400 °C, corresponding to the content of hemicellulose and cellulose degradation, respectively.²²

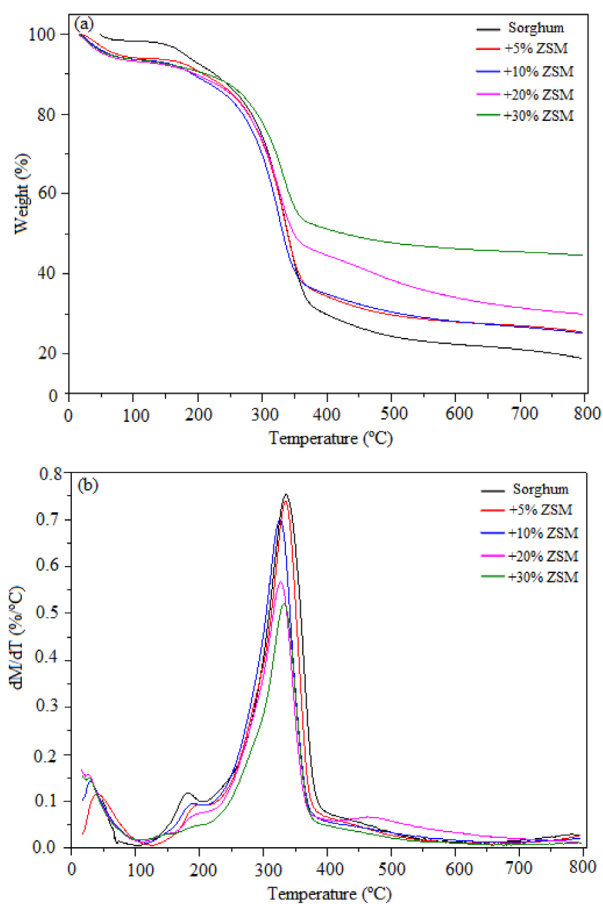


Figure 1. (a) TG and (b) DTG curves in nitrogen atmosphere from biomass sorghum, and sorghum + ZSM-5.

Lignin degrades in a higher temperature range that varies between 200-800 °C. A mass loss is still perceived between 0-100 °C, which can be attributed to the moisture in the samples. It is also observed that, as the amount of catalyst mixed with biomass increases, the residue (biochar) at the end of the process also increases since the amount of catalyst remains the same at the end of the process.

From the thermogravimetric analyses, it was possible to define the temperature used in the pyrolysis process, which was 500 °C, since, at this temperature, all hemicellulose and cellulose would be degraded, and the production of bio-oil would be ceased.

Despite the similarity observed in the degradation profile, it can be seen that there is a decrease in the intensity of the maximum degradation peak referring to cellulose and in the residual amount at the end of the process as the percentage of catalyst increases. This can be explained due to the deoxygenation reactions taking place in the catalyst, which remove oxygen from pyrolysis vapors such as CO, CO₂, and H₂O. The yield of the solid product is increased due to the formation of coke deposits on the surface and in the pores of the catalyst.

Experimental design in fast pyrolysis

The experiments were run after setting the pyrolysis temperature and design parameters. After performing all the experiments, the values of the response variables could be put into the Statistica software. This software analyzes which variables were significant for the desired response (hydrocarbon content) and builds the surface. Table 6 illustrates the response values obtained for the experiments. Figure 2 shows the Pareto chart obtained.

The Pareto chart (Figure 2) shows the influence of the studied factors and their interactions on the reaction system.²⁷ An effect is considered significant when it is greater than the standard error at 95% significance ($p > 0.05$), which is indicated in the vertical line of the graph. Thus, the amount of catalyst proved to be the most significant variable for obtaining a bio-oil with higher hydrocarbon content. Moreover, the variable amount of biomass was also significant for this response and the interaction between it and the amount of catalyst. Therefore, only these two variables were considered to continue the construction of the response surface.

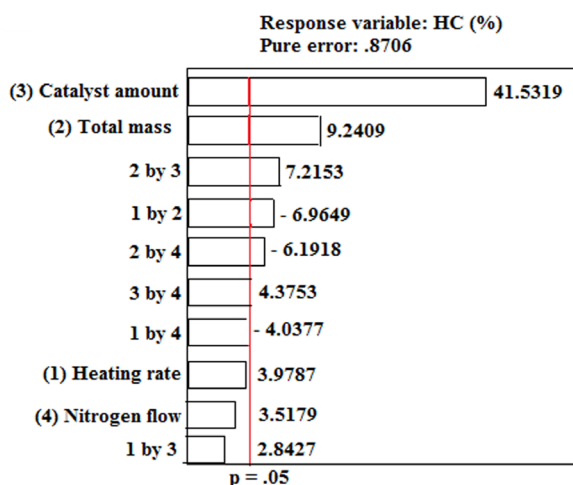
Characterization of bio-oils

FTIR analysis

Figure 3 shows the infrared spectra of the bio-oils from the pure biomass and experiments 7 and 15. They

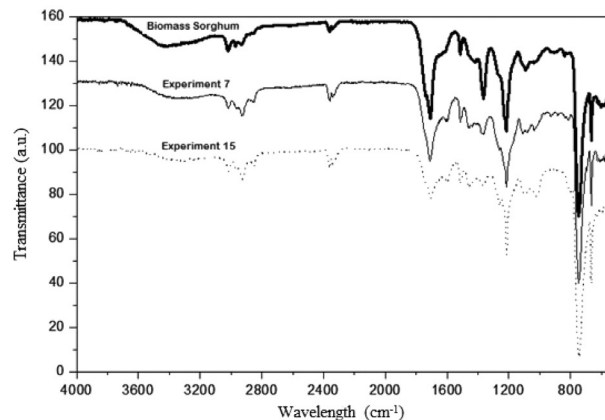
Table 6. Responses obtained from design of experiment for hydrocarbon content

Experiment	Hydrocarbon content / %
1	0.0
2	0.0
3	0.6
4	3.0
5	4.4
6	19.4
7	25.7
8	23.4
9	0.0
10	0.8
11	1.1
12	0.0
13	18.2
14	22.9
15	25.5
16	21.0
17	10.3
18	11.9
19	10.2

**Figure 2.** Pareto chart for hydrocarbon content (HC) in bio-oil from sorghum biomass.

present profiles similar to each other but with some notable differences. There is not a very intense band typical in all three cases in the region of 3600-3200 cm^{-1} , a specific region that indicates the presence of the -OH group in the structure, in this case, characteristic of phenolic compounds. In the region of 2800-3000 cm^{-1} , bands indicate the presence of the functional group -(CH)_n, typical of alkyl, aliphatic, and aromatic compounds, and it is possible to verify a significant difference in the intensity

of these bands for each bio-oil. The bands result from the symmetric (ν_s) and asymmetric (ν_{as}) angular deformation vibration of the -CH₂ and -CH₃ groups, respectively. The bio-oil from pure biomass shows higher intensity in the band at 3005 cm^{-1} , corresponding to the bond stretching (ν) C-H of carbon sp², and lower intensity in the bands located at 2954, 2922, and 2852 cm^{-1} , that are assigned to the bond stretching C-H of the sp³ carbon. With the bio-oils derived from experiments 7 and 15, the opposite occurs, i.e., they present a lower intensity in the band located at 3005 cm^{-1} and higher intensity in the bands corresponding to the C-H bond stretching of the sp³ carbon. The band at 2440 cm^{-1} fits CO₂ present in the atmosphere, common in all three cases. The intense band at 1716 cm^{-1} is attributed to the stretching vibration of the carbonyl (-C=O) of ketones, aldehydes, and carboxylic acids, corresponding to the greater presence of ketonic compounds. It is possible to observe a greater intensity of this band in the bio-oil derived from pure biomass with other bio-oils. The band at 1507 cm^{-1} corresponding to the C-C bond of aromatic compounds is more intense and visible in the bio-oil from pure biomass. The intense bands at 1215 and 740 cm^{-1} correspond to the stretching vibration of the C-O bond of phenolic compounds and the C-H bond of aromatic compounds, respectively.

**Figure 3.** FTIR (ATR) spectra of bio-oils from raw biomass sorghum and experiments 7 and 15.

GC-MS

The chemical characterization of the bio-oils was performed by gas chromatography coupled with mass spectrometry.

Table 7 illustrates the distribution of compounds found in the bio-oil obtained from pure biomass. The use of zeolite as a catalyst in the pyrolysis process shows a tendency to reduce the content of oxygenated compounds in the bio-oil. However, these are still predominant. The hydrocarbons are mostly naphthalenes belonging to the polyaromatic hydrocarbons (PAHs) class.

Table 7. Chemical characterization of bio-oil from pure biomass: molecular formula, group, retention time, area, mean, standard deviation, and relative standard deviation

No.	Name	Molecular formula	Group	Retention time / min	Area / %			Mean	SD	RSD
					P1	P2	P3			
1	3-ethoxy-prop-1-ene	C ₅ H ₁₀ O	alkene	39.033	0.92	0.58	0.83	0.78	0.18	0.23
2	cyclopentanone	C ₅ H ₈ O	ketone	41.758	0.00	0.88	1.40	0.76	0.71	0.93
3	3-furaldehyde	C ₅ H ₄ O ₂	aldehyde	43.442	0.00	0.20	0.24	0.15	0.13	0.88
4	2,5-furandione	C ₄ H ₂ O ₅	ketone	44.850	0.27	0.44	0.49	0.40	0.12	0.29
5	2-cyclopenten-1-one	C ₅ H ₆ O	ketone	45.017	0.90	2.10	2.41	1.80	0.80	0.44
6	furfural	C ₅ H ₄ O ₂	aldehyde	45.283	2.81	4.50	4.94	4.08	1.12	0.28
7	1,2-ethanediol, diacetate	C ₆ H ₁₀ O ₄	ester	47.342	1.30	0.96	1.07	1.11	0.17	0.16
8	3,4-dihydropyran	C ₅ H ₈ O	aromatic ether	50.217	2.14	2.12	2.64	2.30	0.29	0.13
9	2-cyclopenten-1-one, 2-methyl	C ₆ H ₆ O ₂	ketone	51.542	1.50	1.42	1.84	1.59	0.22	0.14
10	ethanone, 1-(2-furanyl)	C ₆ H ₆ O ₂	ketone	51.917	1.39	0.98	1.03	1.13	0.22	0.20
11	2(3H)-furanone, 5-methyl	C ₅ H ₆ O ₂	aromatic ether	52.642	2.55	1.77	1.82	2.05	0.44	0.21
12	3,3-dimethyl-butan-2-one	C ₆ H ₁₂ O	ketone	54.875	0.57	0.65	0.58	0.60	0.04	0.07
13	2-butanone, 1-(acetyloxy)	C ₆ H ₁₀ O ₃	ketone	55.083	0.61	0.43	0.38	0.47	0.12	0.26
14	2-furancarboxaldehyde, 5-methyl	C ₆ H ₆ O ₂	aldehyde	55.750	1.95	2.53	2.84	2.44	0.45	0.19
15	phenol	C ₆ H ₆ O	phenol	57.417	5.51	6.71	8.18	6.80	1.34	0.20
16	3,4-dimethyl-pent-3-en-2-one	C ₇ H ₁₂ O	ketone	57.942	0.48	0.76	0.99	0.74	0.26	0.34
17	3,4-dimethyl-cyclopent-2-en-1-one	C ₇ H ₁₀ O	ketone	58.275	0.00	0.30	0.49	0.26	0.25	0.94
18	6-methyl-hept-3-yne	C ₈ H ₁₄	alcyne	58.683	0.01	0.39	0.63	0.34	0.31	0.91
19	tetrahydro-2furanmethanol	C ₅ H ₁₀ O ₂	alcohol	58.958	1.05	1.62	1.70	1.46	0.35	0.24
20	cyclooctene	C ₈ H ₁₄	alkene	60.217	0.10	0.62	0.54	0.42	0.28	0.67
21	2-cyclopenten-1-one, 2-hydroxy-3-methyl	C ₆ H ₈ O ₂	ketone	60.583	3.66	3.03	3.23	3.31	0.32	0.10
22	2,3-dimethyl-2-cyclopenten-1-one	C ₇ H ₁₀ O	ketone	61.633	0.65	0.98	1.11	0.91	0.24	0.26
23	tetrahydrofurfurylalcohol	C ₅ H ₁₀ O ₂	alcohol	62.542	3.56	1.27	1.35	2.06	1.30	0.63
24	<i>o</i> -cresol	C ₇ H ₈ O	phenol	62.933	1.35	2.62	2.75	2.24	0.77	0.35
25	<i>p</i> -cresol	C ₇ H ₈ O	phenol	64.233	2.61	3.91	4.13	3.55	0.82	0.23
26	4,5-dimethyl-hex-a-en-3-one	C ₈ H ₁₄ O	ketone	64.850	0.47	0.27	0.26	0.33	0.12	0.36
27	guaiacol	C ₇ H ₈ O ₂	phenol	65.408	6.04	7.47	7.14	6.88	0.75	0.11
28	3-ethyl-2-hydroxy-cyclopent-2-en-1-one	C ₇ H ₁₀ O ₂	ketone	67.117	2.06	2.05	1.84	1.98	0.12	0.06
29	3-ethyl-phenol	C ₈ H ₁₀ O	phenol	70.442	5.54	8.17	8.14	7.28	1.51	0.21
30	4-methyl-2-methoxy-phenol	C ₈ H ₁₀ O ₂	phenol	72.217	1.47	2.10	1.88	1.82	0.32	0.18
31	2,3-dihydro-benzofuran	C ₈ H ₈ O	aromatic ether	73.192	23.58	14.66	13.31	17.18	5.58	0.32
32	2-methoxy-4-ethyl-phenol	C ₉ H ₁₂ O ₂	phenol	77.217	2.93	5.30	4.45	4.23	1.20	0.28
33	2-methoxy-4-vinyl-phenol	C ₉ H ₁₀ O ₂	phenol	78.892	9.34	8.75	6.96	8.35	1.24	0.15
34	2,6-dimethoxy-phenol	C ₈ H ₁₀ O ₃	phenol	80.108	8.69	6.35	6.16	7.07	1.41	0.20
35	3-methoxy-4-hydroxy-benzaldehyde	C ₈ H ₈ O ₃	aldehyde	82.358	1.79	0.84	0.75	1.13	0.58	0.51
36	2-methoxy-4-(1-propenyl)-phenol	C ₁₀ H ₁₂ O ₂	phenol	85.050	2.20	2.27	1.50	1.99	0.43	0.21

SD: standard deviation, RSD: relative standard deviation.

Uemura *et al.*³⁵ separately carried out the pyrolysis in the presence and absence of the protonated zeolite of cellulose, hemicellulose, and lignin. It was observed that the major conversion of oxygenated compounds present in the pyrolysis vapors into aromatic and polyaromatic hydrocarbons comes mainly from the compounds derived from cellulose and hemicellulose, where cellulose is the majority. This is explained because the C–O bond between the aromatic ring and the hydroxyl group in the phenol molecules derived from lignin is refractory to zeolite. This also explains the significant presence of phenolic compounds in the bio-oils obtained in this study, even with zeolite.

RSM

Response surface for hydrocarbons

Figure 4 shows the response surface that relates the hydrocarbon content in the bio-oils with the amount of catalyst and biomass used from CCD. Equation 3 shows the function representing this surface.

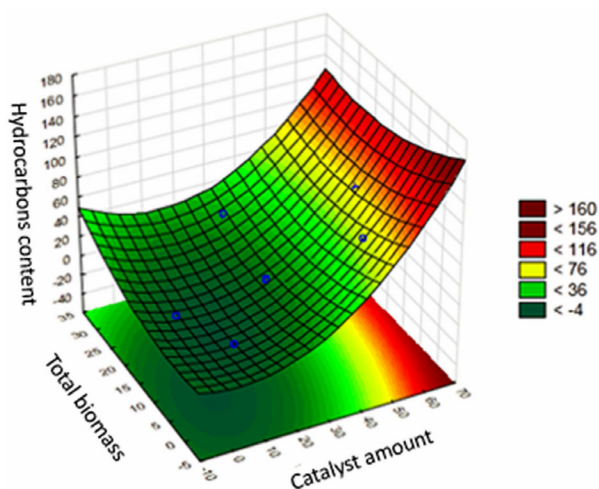


Figure 4. Response surface for the percentage of hydrocarbons present in the bio-oils.

Table 8. Representation of the parameters used to obtain the response surface for hydrocarbons

Factor	Regression coefficient	Pure error	t(1)	p	Confidence interval	
					(-95%)	(+95%)
Intercept	-1.360	1.515	-0.897	0.534	-20.611	17.891
(1) Catalyst amount (L)	-0.282	0.068	-4.124	0.151	-1.154	0.588
Catalyst (Q)	0.034	0.000	35.165	0.018	0.021	0.047
(2) Biomass amount (L)	-0.641	0.137	-4.681	0.133	-2.384	1.100
Biomass (Q)	0.047	0.003	12.182	0.052	-0.002	0.097
1L vs. 2L	-0.024	0.002	-11.426	0.055	-0.050	0.002

t(1): Student's *t*-test with 01 degree of freedom and $p = 0.05$; p : *p*-value 95%.

The quadratic function representing this surface is given by:

$$\hat{y} = -1.360 - 0.283x_1 - 0.642x_2 + 0.034x_1^2 + 0.048x_2^2 - 0.024x_1x_2 \quad (3)$$

where x_1 = catalyst amount (% m/m); x_2 = biomass amount (g); \hat{y} = percentage of hydrocarbon in the bio-oil.

Such a function can be generated from the coefficients obtained by the matrix equations cited above. These are shown in Table 8.

According to Figure 4, there is a critical minimum point where $x_1 = 8.456$ g (biomass amount) and $x_2 = 7.024\%$ m/m (catalyst). This means that even using large amounts of catalyst in the process, it is difficult to favor the formation of hydrocarbons. The data show that, with this biomass in the pyrolytic process, the major forms of oxygenated compounds prevail, partly due to the complexity of the structure of lignocellulosic biomass and the difficulty in promoting deoxygenation reactions.^{35,36} However, there is a curvature that tends to optimal values of hydrocarbon formation, but they are very high values for the parameters evaluated, which in industrial terms, would not be interesting to use since catalysts generally have a high value, generating large costs for industries.

Response surface for phenolic compounds

Since the tendency shown for this process is the production of oxygenated compounds, and since these are primarily phenolic, another response surface was constructed (Figure 5), as these compounds can be used as antioxidants, phenolic resins, solvents, wood preservatives, monomers for plastics, etc.³⁷

The response surface provides a maximum critical point, i.e., the optimal condition of the amount of biomass and catalyst that provides the highest percentage of phenolic compounds in pyrolysis. The quadratic equation (the coefficients again were obtained by matrix equations, Table 9) is given by equation 4:

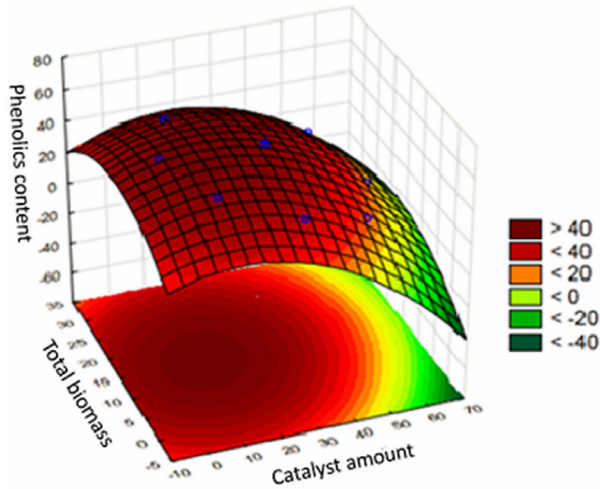


Figure 5. Response surface to a percentage of phenolic compounds in the bio-oil.

$$\hat{y} = 42.783 + 0.418x_1 + 1.759x_2 - 0.020x_1^2 - 0.062x_2^2 + 0.009x_1x_2 \tag{4}$$

where x_1 = catalyst quantity (% m/m); x_2 = biomass quantity (g); \hat{y} = percentage of phenolic compounds in the bio-oil.

Since there is a point of maximum curvature on the surface to obtain the critical point coordinates, each variable’s partial derivative is calculated as a response function and set equal to zero (maximum point) (equations 5 and 6).

Thus:

$$\frac{\partial \hat{y}}{\partial x_1} = 0.418 - 0.04x_1 + 0.009x_2 = 0 \tag{5}$$

$$\frac{\partial \hat{y}}{\partial x_2} = 1.759 - 0.124x_2 + 0.009x_1 = 0 \tag{6}$$

The critical point in the equation designates the response surface of phenolic compounds is $x_1 = 13.88\%$ m/m of catalyst and $x_2 = 15.19$ g of biomass, obtaining the maximum percentage of these compounds present in

the bio-oil. The value of 59.05% (area) of phenols is found. The software Statistica predicts the values of $x_1 = 13.47\%$ m/m of catalyst, $x_2 = 15.20$ g of biomass and 58.96% (area) of phenols. Thus, comparing the two results, they are remarkably close and a good fit for this quadratic function.

Conclusions

The use of a unique critical quality attribute (CQA) throughout the pyrolytic process (zeolite, ZSM-5) by using a 2^4 full factorial design, followed by optimization through a response surface methodology (RSM) based on CCD involving samples of biomass sorghum BRS716 (*Sorghum bicolor* L. Moench) showed a different composition of bio-oil obtained from catalytic pyrolysis of this biomass.

The results obtained in this study showed the potential use of sorghum biomass as an alternative renewable source to fossil fuels for industrial applications. In addition, it was possible to realize that the bio-oil obtained through pyrolysis with this biomass is rich in oxygenated compounds; the majorities are phenolic compounds, which have potential use in biorefinery industries, such as in the production of phenolic resins.

The design results made it possible to create a response surface using CCD, searching for the best condition of catalyst and biomass (optimal point) to obtain the best product. Thus, it was possible to create a response surface from these two variables (biomass and catalyst), in which a minimum critical point was reached. The production of a bio-oil rich in hydrocarbon compounds is possible, but a large amount of catalyst was required because the hydrocarbon content increases when the catalyst concentration also increases from 5 to 30% m/m.

The response surface provides a maximum critical point, i.e., the optimal condition of the amount of biomass and catalyst that provides the highest percentage of phenolic compounds in pyrolysis. Thus, obtaining the maximum

Table 9. Representation of the parameters used to construct the response surface for phenolic compounds

Factor	Regression coefficient	Pure error	t(1)	p	Confidence interval	
					(-95%)	(+95%)
Intercept	42.783	0.547	78.144	0.008	35.826	49.739
(1) Amount of catalyst (L)	0.417	0.024	16.860	0.037	0.102	0.732
Amount of catalyst (Q)	-0.020	0.0003	-57.411	0.011	-0.024	-0.015
(2) Amount of biomass (L)	1.758	0.0495	35.489	0.017	1.129	2.388
Amount of biomass (Q)	-0.061	0.0014	-43.382	0.014	-0.079	-0.043
1L vs. 2L	0.008	0.0007	11.428	0.055	-0.0009	0.018

t(1): Student’s *t*-test with 01 degree of freedom and $p = 0.05$; p : *p*-value 95%.

rate of these compounds present in the bio-oil, the value of 59.05% (area) of phenols is found.

Once a larger fraction of catalyst weight than biomass is needed, it turns the technical feasibility of the pyrolysis process at a large scale very low. Once again, the RSM could be useful to find a practical zeolite concentration in biomass.

Supplementary Information

Supplementary data are available free of charge at <http://jbcbs.sbg.org.br> as PDF file.

Acknowledgments

The authors would like to thank FINEP-Pluricana (22.17.00.012.00.00), BNDES (17.2.046.1) and Instituto Nacional de Ciências e Tecnologias Analíticas Avançadas (INCTAA, CNPq - 465768/2014-8) for the financial support of this project.

Author Contributions

Diego M. Costa was responsible for the experimental work and methodology, writing original draft, interpretation of results, and writing/reviewing; Isabel C. P. Fortes for the supervision, interpretation of results, writing/reviewing, conceptualization and funding acquisition; Maria L. F. Simeone for the conceptualization, experimental work, and writing/reviewing; Rafael A. C. Parrella for the raw material preparation and funding acquisition.

References

1. Stamenkovic, O. S.; Siliveru, K.; Veljkovic, V. B.; Bankovic-Ilic, I. B.; Tasic, M. B.; Ciampitti, I. A.; Dalovic, I. G.; Mitrovic, P. M.; Sikora, V. S.; Prasad, P. V. V.; *Renewable Sustainable Energy Rev.* **2020**, *124*, 109769. [Crossref]
2. Shen, D. K.; Jin, W.; Hu, J.; Xiao, R.; Luo, K. H.; *Renewable Sustainable Energy Rev.* **2015**, *51*, 761. [Crossref]
3. Bai, X. L.; Kim, K. H.; Brown, R. C.; Dalluge, E.; Hutchinson, C.; Lee, Y. J.; Dalluge, D.; *Fuel* **2014**, *128*, 170. [Crossref]
4. Mettler, M. S.; Vlachos, D. G.; Dauenhauer, P. J.; *Energy Environ. Sci.* **2012**, *5*, 7797. [Crossref]
5. Ohlrogge, J.; Allen, D.; Berguson, B.; DellaPenna, D.; Shachar-Hill, Y.; Stymne, S.; *Science* **2009**, *324*, 1019. [Crossref]
6. McKendry, P.; *Bioresour. Technol.* **2002**, *83*, 37. [Crossref]
7. de Almeida, L. G. F.; Parrella, R. A. C.; Simeone, M. L. F.; Ribeiro, P. C. O.; dos Santos, A. S.; da Costa, A. S. V.; Guimaraes, A. G.; Schaffert, R. E. C.; *Biomass Bioenergy* **2019**, *122*, 343. [Crossref]
8. Wilhelm, W. W.; Johnson, J. M. F.; Hatfield, J. L.; Voorhees, W. B.; Linden, D. R.; *Agron. J.* **2004**, *96*, 100. [Crossref]
9. Barrière, Y.; Riboulet, C.; Mechin, V.; Maltese, S.; Pichon, M.; Cardinal, A.; Lapiere, C.; Lübberstedt, T.; Martinant, J. P.; *Genes, Genomes Genomics* **2007**, *1*, 133. [Link] accessed in July 2022
10. da Silva, M. J.; Carneiro, P. C. S.; Carneiro, J. E. S.; Damasceno, C. M. B.; Parrella, N. N. L. D.; Pastina, M. M.; Simeone, M. L. F.; Schaffert, R. E.; Parrella, R. A. C.; *Ind. Crops Prod.* **2018**, *125*, 379. [Crossref]
11. Robak, K.; Balcerek, M.; *Microbiol. Res.* **2020**, *240*, 126534. [Crossref]
12. Bridgwater, A. V.; Peacocke, G. V. C.; *Renewable Sustainable Energy Rev.* **2000**, *4*, 1. [Crossref]
13. Bridgwater, A. V.; Meier, D.; Radlein, D.; *Org. Geochem.* **1999**, *30*, 1479. [Crossref]
14. Sharma, A.; Shinde, Y.; Pareek, V.; Zhang, D.; *Bioresour. Technol.* **2015**, *198*, 309. [Crossref]
15. Sarker, T. R.; Nanda, S.; Dalai, A. K.; Meda, V.; *BioEnergy Res.* **2021**, *14*, 645. [Crossref]
16. Zhang, L.; Liu, R. H.; Yin, R. Z.; Mei, Y. F.; *Renewable Sustainable Energy Rev.* **2013**, *24*, 66. [Crossref]
17. Ponjavic, M.; Karabegovic, A.; Custovic, H.; Hivzievendic, J.; *Int. J. Sustainable Energy* **2021**, *40*, 654. [Crossref]
18. Yin, R. Z.; Zhang, L.; Liu, R. H.; Mei, Y. F.; Yu, W. J.; *Fuel* **2016**, *170*, 1. [Crossref]
19. Zhao, Y.; Deng, L.; Liao, B.; Fu, Y.; Guo, Q. X.; *Energy Fuels* **2010**, *24*, 5735. [Crossref]
20. Yildiz, G.; Pronk, M.; Djokic, M.; van Geem, K. M.; Ronsse, F.; van Duren, R.; Prins, W.; *J. Anal. Appl. Pyrolysis* **2013**, *103*, 343. [Crossref]
21. Taarning, E.; Osmundsen, C. M.; Yang, X. B.; Voss, B.; Andersen, S. I.; Christensen, C. H.; *Energy Environ. Sci.* **2011**, *4*, 793. [Crossref]
22. Liu, C. J.; Wang, H. M.; Karim, A. M.; Sun, J. M.; Wang, Y.; *Chem. Soc. Rev.* **2014**, *43*, 7594. [Crossref]
23. Vichaphund, S.; Aht-ong, D.; Sricharoenchaikul, V.; Atong, D.; *Renewable Energy* **2014**, *65*, 70. [Crossref]
24. Kim, J. Y.; Lee, J. H.; Park, J.; Kim, J. K.; An, D.; Song, I. K.; Choi, J. W.; *J. Anal. Appl. Pyrolysis* **2015**, *114*, 273. [Crossref]
25. Barros Neto, B.; Scarminio, I. S.; Bruns, R. E.; *Como Fazer Experimentos. Pesquisa e Desenvolvimento na Ciência e na Indústria*; Editora Unicamp: Campinas, 2002.
26. Van Soest, P. J.; *Nutritional Ecology of the Ruminant*; Cornell University Press: Ithaca, 1994.
27. Barros Neto, B.; Scarminio, I. S.; Bruns, R. E.; *Planejamento e Otimização de Experimentos*; Editora Unicamp: Campinas, 1996.
28. *Statistica (Data Analysis Software System)*, version 7; StatSoft, Inc., USA, 2004.
29. Price, B.; *Robust Planning and Analysis of Experiments*; Springer-Verlag: New York, 1997.
30. Leng, L. J.; Yuan, X. Z.; Huang, H. J.; Shao, J. G.; Wang, H.;

- Chen, X. H.; Zeng, G. M.; *Appl. Surf. Sci.* **2015**, *346*, 223. [Crossref]
31. Maldhure, A. V.; Ekhe, J. D.; *Chem. Eng. J.* **2011**, *168*, 1103. [Crossref]
32. Pimentel, L. D.; Batista, V. A. P.; de Barros, A. F.; Teófilo, R. F.; dos Santos, L. A.; *Pesq. Agropec. Trop.* **2017**, *47*, 424. [Crossref]
33. Singh, M. P.; Erickson, J. E.; Sollenberger, L. E.; Woodard, K. R.; Vendramini, J. M. B.; Fedenko, J. R.; *Biomass Bioenergy* **2012**, *47*, 1. [Crossref]
34. de Oliveira, A. A.; Pastina, M. M.; de Souza, V. F.; Parrella, R. A. C.; Noda, R. W.; Simeone, M. L. F.; Schaffert, R. E.; de Magalhães, J. V.; Damasceno, C. M. B.; Margarido, G. R. A.; *Mol. Breed.* **2018**, *38*, 49. [Crossref]
35. Uemura, K.; Appari, S.; Kudo, S.; Hayashi, J.; Einaga, H.; Norinaga, K.; *Fuel Process. Technol.* **2015**, *136*, 73. [Crossref]
36. Liu, J.; Hou, Q.; Ju, M.; Ji, P.; Sun, Q.; Li, W.; *Catalysts* **2020**, *10*, 742. [Crossref]
37. Vu, H. P.; Nguyen, L. N.; Vu, M. T.; Johir, M. A.; McLaughlan, R.; Nghiem, L. D.; *Sci. Total Environ.* **2020**, *743*, 140630. [Crossref]

Submitted: April 9, 2022

Published online: July 4, 2022

